

A Parametric Study on Welding Process Simulation for Multi-pass welds in a Plate

Won Dong Park^a, Chi Bum Bahn^{a*}, Ji Hun Kim^a

^aPusan National University, 2, Busandaehak-ro 63beon-gil, Geumjeong-gu, Busan 609-735, Republic of Korea

*Corresponding author: bahn@pusan.ac.kr

1. Introduction

Many attempts have been made to predict weld residual stress using finite element analysis (FEA) models. However, FEA results also have considerable deviations depending on applied assumptions and boundary conditions, which is basically due to the inherent complex characteristic of the weld residual stress determined by various factors. EPRI (MRP-316, 317)^(1,2) and USNRC (NUREG-2162)⁽³⁾ have performed related studies for FEA models to predict the weld residual stress distribution. In this work, a systematic parametric study was performed to find out how major assumptions and conditions used in the simulation could affect the weld residual stress distribution. 2-dimensional simulation was conducted by using commercial FEA software, ABAQUS⁽⁴⁾, for multi-pass Alloy 82 welds performed in a stainless steel plate (EPRI MRP-316, P-4, phase 1).

2. Finite Element Analysis Model and Process

In this work, FEA modeling of multi-pass welds is shown and residual stress FEA process is described.

2.1 Finite element modeling of the multi-pass welds

A plate model (phase 1, P-4) performed by EPRI MRP-316⁽¹⁾ and NUREG-2162⁽³⁾ was chosen for a finite element thermal-structure analysis.

Fig. 1 shows the overall shape of parts and constraint conditions. Finite element model consists of welds (alloy 82), parent (316 stainless steel) and fixture backing plate (aluminum).

Thermocouple locations are also shown. Three thermocouples were attached on the topside of the plate to record temperatures and two thermocouples were attached to the underside of the plate immediately adjacent to one another for redundancy.

Properties of alloy 82 and 316 stainless steel were taken from MRP-317⁽²⁾. To simulate the mixed kinematic hardening behavior Lemaitre Chaboche formulation factors were entered to property table⁽⁵⁾.

A 4-node linear heat transfer quadrilateral element type (DC2D4) was used for the transient thermal analysis and a 4-node bilinear plane strain quadrilateral, reduced integration element type (CPE4R) was used for the structural analysis.

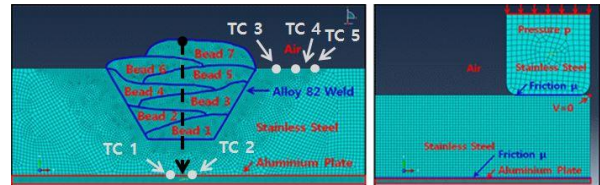


Fig. 1. Finite element model for weld residual stress analysis.

2.2 Thermal analysis

By using “predefined fields” option in ABAQUS 2016, a result of thermal analysis was put into the structure analysis model as the initial condition every increment (a sequentially coupled temperature-stress procedure)⁽⁶⁾. By using model change option of ABAQUS, all of welds were stacked sequentially on pre-deposited welds⁽⁷⁾. After applying heat to a specific bead, welds and parent were cooled down sufficiently (for 3000 sec). in conduction and convection conditions. The surfaces exposed to the air were considered as being a natural convection condition ($h= 10, 25 \text{ W/m}^2\cdot\text{°C}$, $T_s= 21.1 \text{ °C}$)

There are two methods to apply heat to welds. First, heat input method is simulated by power density (q , J/s/mm^3) using the following equation (1)⁽²⁾.

$$q = Ke^{-\frac{3t^2}{a^2}} \left(K = \sqrt{\frac{3}{\pi}} \times \frac{E \cdot V \cdot A}{A_w}, a = \frac{L}{S} \right) \quad (1)$$

q =power density (J/s/mm^3), t =time from start of weld, L =characteristic length (mm), S =torch travel speed (mm/s), E =scaling coefficient, $V \cdot A$ =welding power(J/s), A_w =weld volume(mm^3) = weld cross section area(mm^2) times unit depth(mm).

Amounts of heat input were calculated and variable values were taken from the MRP-317 report ($L= 25.4 \text{ mm}$, $S= 1.48 \text{ mm/s}$, $V \cdot A= 225 \cdot 11.5 \text{ J/s}$, $E= 1.224$)⁽²⁾.

Applied amount of power density is presented in Fig. 2.

Second, predefined temperature method ($T_{pre} : 1800 \text{ °C}$ or 1900 °C , for 0.675 sec) is to set up high temperature over the melting point and deactivate welds until the welds are actually deposited by using model change option of ABAQUS.

Once the weld is deposited and activated, weld starts to cool down rapidly. However, it doesn't have additional heat sources in contrast with power density method. For this reason, welds and parent were cooled

down more rapidly than power density method as soon as they are deposited.

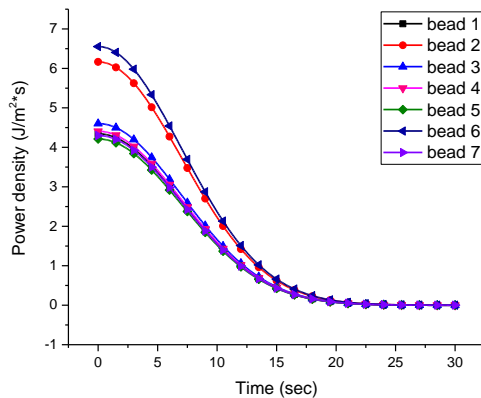


Fig. 2 Applied power density vs time on welds

Major factors determining cooling rates of welds are material's thermal conductivity, convective heat transfer coefficient and thermal conductance. Table 1 shows assumed major boundary surfaces thermal conditions.

To compare with the effect of natural convective heat transfer coefficient, constant values are assumed to $10^{(8)}$, $25 \text{ W/m}^2 \cdot ^\circ\text{C}$ at room temperature (21.1°C), respectively. However, convective heat transfer coefficients are associated with the surface temperature. Following equation 2⁽⁸⁾ shows the bilinear relationship of convective heat transfer coefficient and temperature.

Table I: Major boundary surface thermal conditions.

Boundary surface	Convective heat transfer coefficient ($\text{W/m}^2 \cdot ^\circ\text{C}$)	Conductance ($\text{W}/^\circ\text{C}$)
Welds – air	(1) $10^{(8)}$	
Parents –air	(2) 25	
	(3) Equation 2 ⁽⁸⁾	
Parents- aluminum		100, 250
Aluminum - table		$800^{(9)}$

$$h \left(\frac{\text{W}}{\text{m}^2 \cdot ^\circ\text{C}} \right) = 0.668 T \quad \text{for } 0 \leq T \leq 500^\circ\text{C} \quad (2)$$

$$0.231T - 82.1 \quad \text{for } T \geq 500^\circ\text{C}$$

In actually, because of weld expansion and shrink phenomenon, the distance of parent and aluminum plate surface is irregular. For this reason, the unstable thermal transfer happens. As discontinuous heat transfer makes difficulties to simplifying analysis process, this matter could be simple by assuming heat sink compound between two surfaces. In this work, conductance of surfaces between parent and aluminum 100, 250 $\text{W}/^\circ\text{C}$ and aluminum-table were set to 800 $\text{W}/^\circ\text{C}$.

2.3 Structural analysis

A result of thermal analysis were put into the structure analysis model as initial conditions every increment. Block dumped modeling method has advantages to minimizing the analysis size and computer resources. However, in case of deformation of welds and parent after welding process are bigger than structural acceptance criteria, not only welds were overlapped but inaccurate results were produced.

In this work, method of EPRI⁽¹⁾ and B. Brickstad, B. L. Josefson⁽⁸⁾ were applied to avoid this problem. Until the activation of the specific weld, deactivated welds have a low stiffness, a very low yield stress and thermal strain free at “softening temperature (in this case, $T_{\text{soft}} = T_{\text{melt}}$),” to make more flexible nodal displacement

Additionally, by considering isotropic hardening, behavior and annealing effect ($T_{\text{anneal}} = T_{\text{solidus}}$), distribution of the residual stress on welds in a centerline could be estimated.

3. Results

By comparing with calculated temperature data in the finite element analysis and measured temperature data of MRP-316 report, realistic boundary conditions could be estimated.

Fig. 3 shows temperature histories at the location of TC 1 according to the different thermal conductance (100, 250 $\text{W}/^\circ\text{C}$) and convective heat transfer coefficient ($h = h(T)$, $h = 10$ and $100 \text{ W/m}^2 \cdot ^\circ\text{C}$) in case of power density method.

Meanwhile, Fig .4 shows temperature histories at the location of TC 1 according to the different methods to apply heat to welds under the same boundary conditions.

Although peak temperature was higher than MRP-316, insufficient heat have been added to welds in case of the predefined temperature methods.

From the results, it seems that thermal conductance of parents-aluminum boundary surface and peak temperature are more influential than convective heat transfer coefficient in high temperature region. However, convective heat transfer coefficient also is important to determine the subtle temperature changes in the low temperature region.

Although there are seven pass and five locations of thermocouple, data from thermocouple 1 and 3 were compared with data of MRP-316 report representatively.

Since weld's real shape are different each other and heat input are irregular, it is difficult to fit temperature history perfectly. For this reason, peak temperature and cooling curve could be major comparison factors. Table 2 shows the difference of measured and estimated peak temperature. Although it has a margin of error, power density method has a more realistic peak temperature and cooling curve than predefined temperature method.

Before to comparing FEA results in various welding conditions, a number of repeated analyses were tried to

adjust peak temperature and cooling curve to MRP-316 as possible.

Finally, thermal conductance and convective heat transfer coefficient were determined to 100 W/°C and equation 2 ($h = h(T)$), respectively.

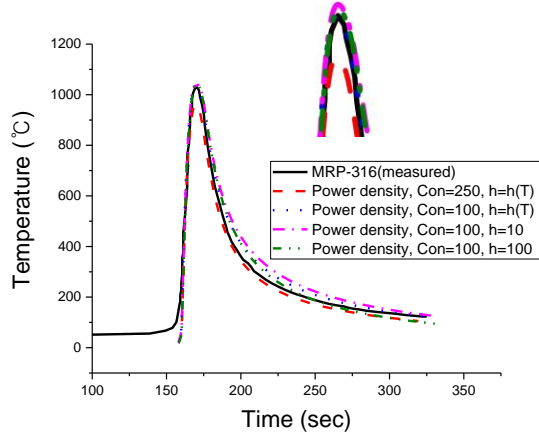


Fig. 3 Temperature histories at the position of TC 1 according to the thermal conductance and convective heat transfer coefficient.

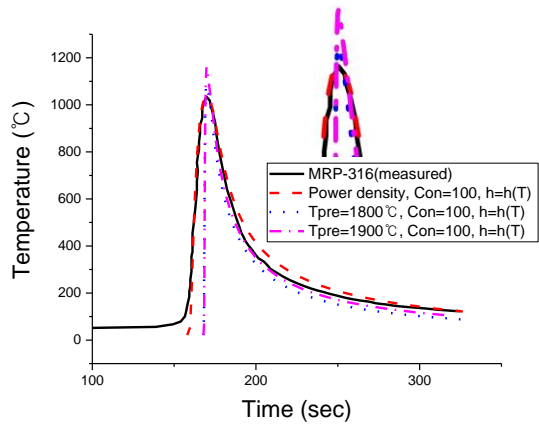


Fig. 4 Temperature changes at the position of TC 1 applied the heat input methods.

Table II: Maximum temperature at thermocouple 1 and 3 for a welding process (conductance 100 W/°C).

TC1 (°C)	Measured	Estimated		
	MRP-316 Data ⁽¹⁾	Power Density	Predefined Temperature	
			1800 °C	1900 °C
Pass1	1034	1035 (+0.1%)	1084 (+4.8%)	1161 (+12.3%)
Pass2	785	859(+9.4%)	668(-14.9%)	712(-9.3%)
Pass3	630	640(+1.6%)	537(-14.8%)	572(-9.2%)
Pass4	542	571(+5.4%)	481(-11.3%)	514(-5.2%)
Pass5	443	481(+8.6%)	368(-16.9%)	393(-11.3%)
TC3				
Pass1	359	440	330	356

		(+22.6%)	(-8.1%)	(-0.8%)
Pass2	280	295(+5.4%)	176(-37.1%)	192(-31.4%)
Pass3	566	552(-2.5%)	503(-11.1%)	536(-5.3%)
Pass4	307	281(-8.5%)	217(-29.3%)	235(-23.5%)
Pass5	636	551(-13.4%)	525(-17.5%)	562(-11.6%)

Fig. 5 and 6 shows annealing effect on final weld residual stresses in isotropic hardening behavior and loose constraint condition. Results of MRP-316 model B and C (annealed, isotropic hardening) were purposed to compare with ours. Although deposited weld shapes are different each other, distributions of stress show similar tendency.

For reference, the bottom of the plate weld groove cavity is located at 10 mm from the top of the plate.

Maximum transverse stress (S11) is slightly reduced in Fig. 5 and longitudinal stresses of welds region (S33) are also decreased considerably in Fig. 6. It seems that residual stresses were partially reduced by the annealing effect.

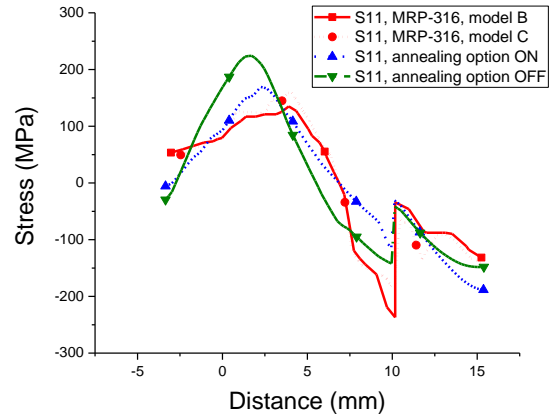


Fig. 5 Distribution of the final transverse direction residual stress (S11) depending on the annealing effect.

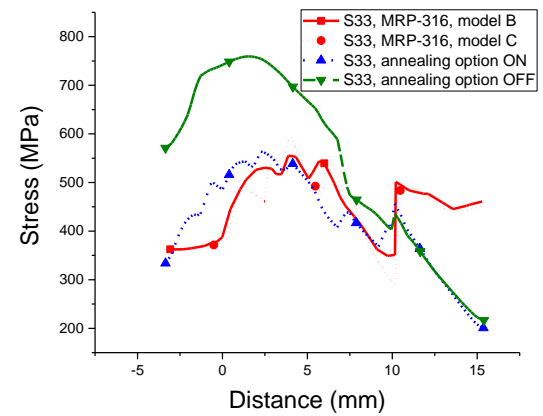


Fig. 6 Distribution of the final longitudinal direction residual stress (S33) depending on the annealing effect.

However it is ambiguous to say annealing effect reduces residual stress throughout the thickness.

In this work, it was assumed that the annealing effect occur a sudden phenomenon at specific temperature ($T_{\text{anneal}} = T_{\text{solidus}}$).

However the annealing effect occurs gradually in high temperature region. Therefore, to clarify the annealing effect on weld residual stress more realistic, it needs to be performed more detailed analyses by dividing annealing region into two or more.

Fig. 7 and 8 shows the final weld residual stresses depending on different heat input methods in isotropic hardening behavior and loose constraint condition.

Annealing effect was considered to all of case.

Maximum residual stress was decreased on the welds as predefined temperature increases.

Although shape of welds is slightly different each other, all of cases tend to have similar distribution on welds generally.

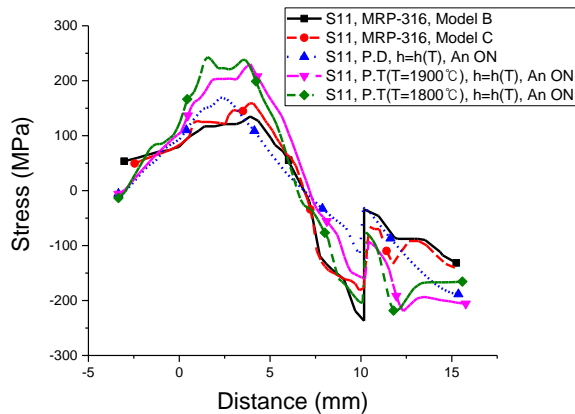


Fig. 7 Distribution of the final transverse direction residual stress (S11) depending on heat input methods.

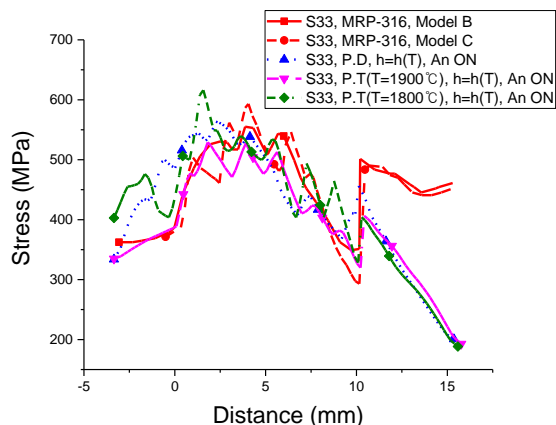


Fig. 8 Distribution of the final longitudinal direction residual stress (S33) depending on heat input methods.

4. Conclusions

From the previous results, we could make the following conclusions.

1. The method of applying power density is more realistic than predefined temperature.
2. It seems that annealing effect reduces the transverse direction weld residual stress (S33). However more detailed analyses for annealing effect are needed.
3. Although heat input methods are different, all of cases tend to have similar distribution on welds.

Acknowledgements

This work was supported by the Nuclear Safety Research Program through the Korea Foundation Of Nuclear Safety(KOFONS), granted financial resource from the Nuclear Safety and Security Commission(NSSC), Republic of Korea (No. 1403006)

REFERENCES

- [1] B roussard, J., Materials Reliability Program: Finite-Element Model Validation for Dissimilar Metal Butt-Welds (MRP-316, Revision 1): Volumes 1 and 2, EPRI, Palo Alto, CA, 2015.
- [2] Broussard, J., Material reliability program: welding residual stress dissimilar Metal butt-weld finite element modeling handbook (MRP-317, Revision 1), EPRI, Palo Alto, CA, 2015.
- [3] Benson, M., Rudland, D. J., & Csontos, A., 2014, Weld Residual Stress Finite Element Analysis Validation: Part 1, Data Development Effort, United States Nuclear Regulatory Commission.
- [4] Simulia., ABAQUS 2016 User's Manuals. Ver.2016, 2016.
- [5] Paul Crooker., Weld residual stress finite element analysis validation introduction and overview, EPRI, 17-22, 2011.
- [6] Kim, Jong-Sung, Myoung-Soo Ra, and Kyoung-Soo Lee., Investigation on the effects of geometric variables on the residual stresses and PWSCC growth in the RPV BMI penetration nozzles, Journal of Mechanical Science and Technology 29.3, 1049-1064, 2015.
- [7] Elcoate, C. D., et al., Three dimensional multi-pass repair weld simulations, International Journal of Pressure Vessels and Piping 82.4, 244-257, 2005.
- [8] Brickstad, Björn, and B. L., Josefson, A parametric study of residual stresses in multi-pass butt-welded stainless steel pipes, International Journal of Pressure Vessels and Piping, 75.1, 11-25, 2008.
- [9] Eisazadeh, H., et al., Effect of material properties and mechanical tensioning load on residual stress formation in GTA 304-A36 dissimilar weld, Journal of Materials Processing Technology 222, 344-355, 2015.